

*Full Length Research Paper*

# Hydrocarbon trapping mechanism and petrophysical analysis of Afam field, offshore Nigeria

Kehinde D. Oyeyemi\* and Ahzegbobor P. Aizebeokhai

Department of Physics, College of Science and Technology, Covenant University, Nigeria.

Received 5 February, 2015; Accepted 18 March, 2015

The structural trapping mechanism and petrophysical attributes of Afam field, offshore Niger Delta was evaluated using 3D seismic reflection data and composite well logs data. The structure maps and seismic sections show that the anticlinal structure at the centre of the field, which is tied to the crest of the rollover structure assisted by faults, is the principal structure responsible for the hydrocarbon entrapment in the field. Distinctive fault closures are the dominant structural plays in the field. Structural highs, fault assisted closures comprising two-way closure and four-way dip closed structures are evident on the depth structure maps. Petrophysical analysis of four mapped reservoir sand horizons quantitatively revealed water saturation ranging from 3.07 to 12.02% in Well1 and 7.25 to 19.32% in Well 5; hydrocarbon saturation with range 87.98 to 96.93% (well 1), 80.68 to 92.75% (well 5). The porosity and permeability values of the reservoirs within the field proved them to be quite prolific with the porosity ranging from 24.5 to 31% (well 1), 21.25 to 28.25% (well 5) and permeability range of 2606.91 to 11,777.71 mD (well 1), 1050 to 6502.20 mD (well 5).

**Key words:** Niger Delta, trapping mechanism, petrophysical analysis, structural highs, fault assisted closures.

## INTRODUCTION

The ubiquitous economic constraints of developing offshore fields demand assessment of essential reservoir characteristics at the earliest possible opportunity. Characterization of the reservoir sands through petrophysical logs interpretation is quite useful and essential tool for selecting, planning and implementing operationally sound supplementary schemes. Integration of the seismic reflection data and well logs suites are commonly used in exploration for reservoir sands correlation, isopach and structural mappings. They are also useful for the estimation of certain physical properties of the subsurface geology such as the

porosity, permeability, litho-facie characterization and possibly pore geometry. Recovery from producing fields on the other hand can be enhanced significantly through the more gradual process of production monitoring in combination with detailed reservoir modelling and simulations. These efforts continued from the early development stage until a reservoir has reached its economic limits. The integration of geophysical, petrophysical and reservoir engineering data is the key to designing realistic dynamic reservoir models. In the early stage of field appraisal, the emphasis is on detailed seismic analysis combined with geological modelling with

\*Corresponding author. E-mail: [kdoyeyemi@yahoo.com](mailto:kdoyeyemi@yahoo.com), [kehinde.oyeyemi@covenantuniversity.edu.ng](mailto:kehinde.oyeyemi@covenantuniversity.edu.ng)  
Author(s) agree that this article remain permanently open access under the terms of the [Creative Commons Attribution License 4.0 International License](https://creativecommons.org/licenses/by/4.0/)

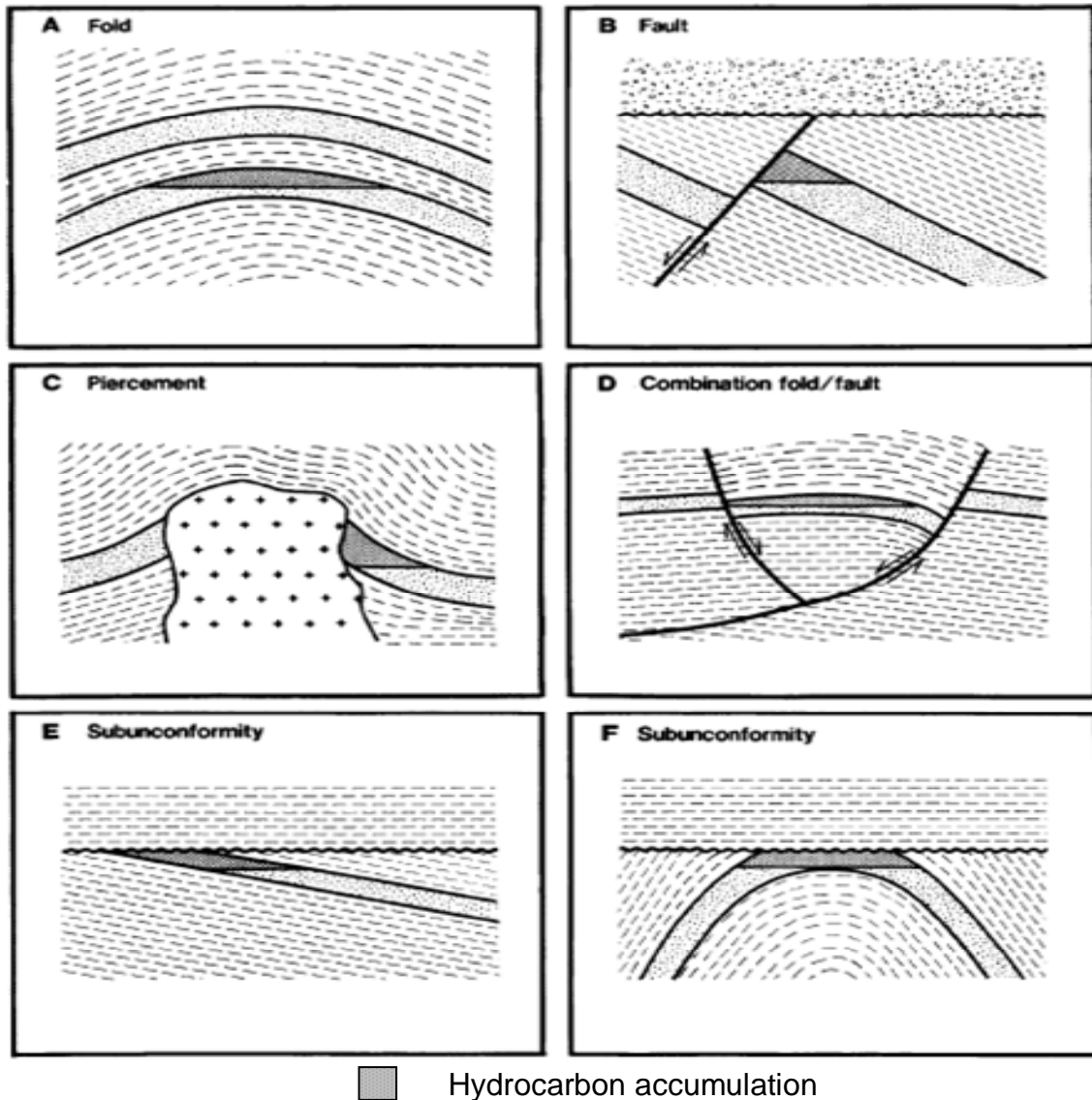


**Figure 1.** Major categories of structural traps: (A) Fold, (B) Fault, (C) Piercement, (D) Combination Fold-Fault, (E) and (F) Subunconformities. The situation in (E), that is, pinchout is usually excluded from structural category (Modified after Biddle and Wielchowsky, 1994).

the aim of delineating structures, faulting and reservoir architecture.

Evaluation of the trapping styles is fundamental in the analysis of a prospect and an essential part in any successful oil and gas exploration program or resource assessment program. A trap is any geometrical arrangement of rock that allows the significant accumulation of oil or gas or both in the subsurface (North, 1985). For a trap to be effective, there are several factors that must be in place including adequate reservoir rocks, seals and timing of the trap-forming process in relation to the hydrocarbon migration. The variability of these factors has led to many different trap classifications by several authors (Clapp, 1929; Levorsen, 1967;

Perrodon, 1983; North, 1985). Structural traps similar to those localised in Niger Delta petroleum province are products of syn-to-post depositional deformation of strata into geometrical structure that permits the accumulation of hydrocarbons in the subsurface. Varieties of schemes have been used to propose subdivisions of structural traps (Figure 1). Clapp (1929) distinguished between anticlinal, synclinal, homoclinal, quaquaversal and fault-dominated traps. Harding and Lowell (1979) used the concept of structural styles, emphasising basement involvement or non-involvement, inferred deformational force and mode of tectonics transport. Perrodon (1983) categorized structural traps into those caused by folding, faulting, fracturing, intrusion and combinations of these

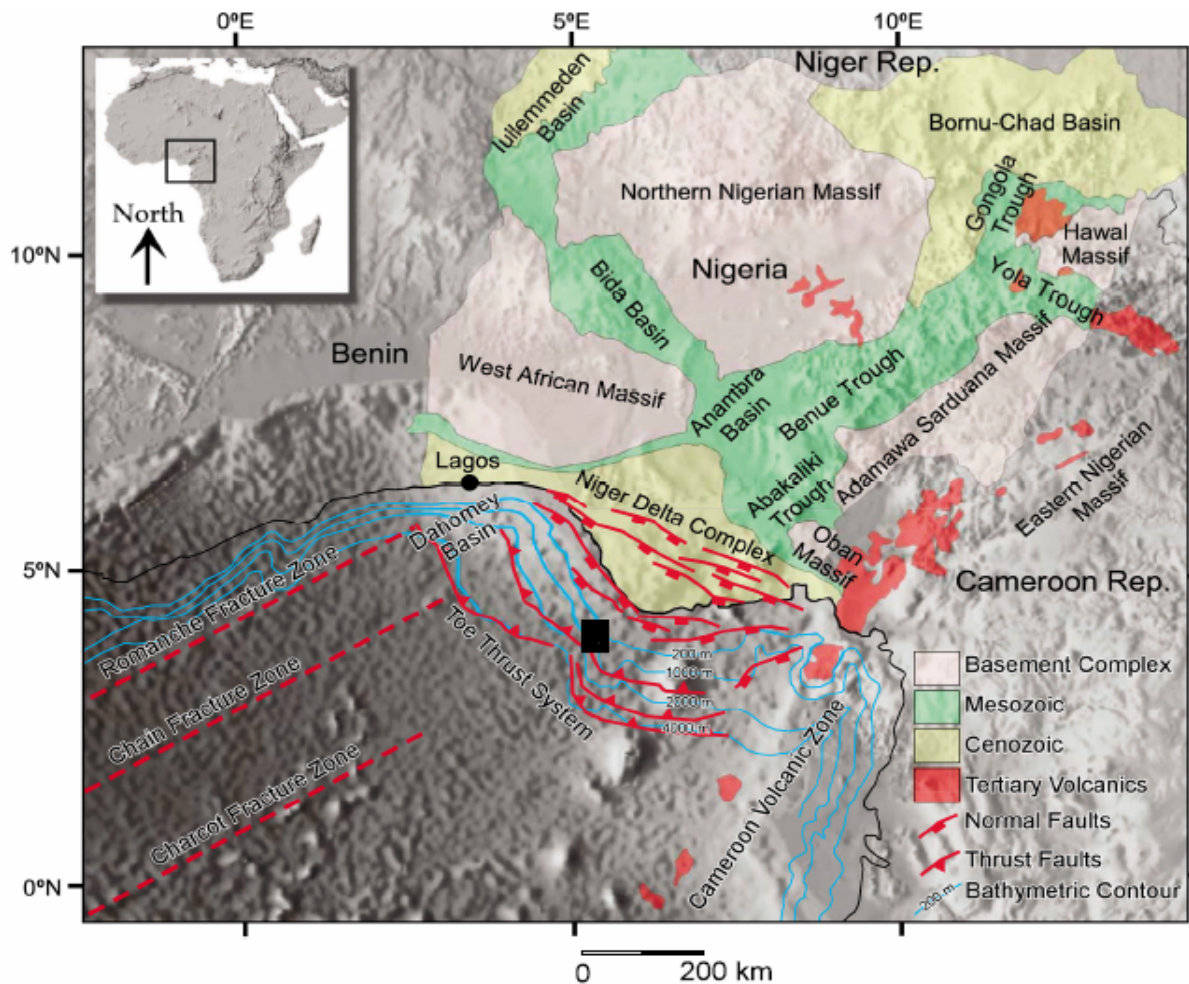


Figure 2. Map of Niger Delta showing the study area.

processes. North (1985), focusing on fold-dominated traps, distinguished between the buckle or thrust-fold, bending fold and immobile convexity traps. Most of the oil field structures and associated traps styles in the Niger Delta have been sufficiently discussed by Weber and Dakoru (1975), Doust and Omatsola (1990), Ojo (1996), Opara and Onuoha (2009) and Reijers (2011).

The study area is offshore Niger Delta and the research is carried out to determine the trapping style and petrophysical attributes evaluation in this field. The abundant evidence of structural traps, good quality reservoir sands and hydrocarbon indicators make the area particularly attractive exploration target. The trapping styles in the field include anticlinal dip closures, upthrown fault (footwall closures) and downthrown fault (hanging wall closures).

#### Location and geological setting of the field

Afam field is situated in the offshore of the Cenozoic

Niger Delta (Figure 2). The deposits in Niger Delta are Tertiary age siliclastic which are attributed to three lithostratigraphic formations, namely Akata, Agbada and Benin Formations. The Akata Formation (marine shale) is characterized by uniform pro-delta shale, which generally is dark grey and medium hard with flora fossils in its upper part. The Akata Formation likely extends to the basement rock. Overlying this formation is the Agbada Formation which is over 10,000 ft thick and range from Eocene in the north to Pliocene in the south and recent in the delta surface. Agbada Formation forms paralic sequence comprises of the oil and gas reservoirs of the Niger Delta, and is composed of the intercalations of sandstone and shale bedsets representing the delta front, distributaries channel and the deltaic plain. The increasing quantities of the sandstone content from the lower part to the upper part connote the seaward advance of the Niger Delta over some periods of geologic time. The continental plain sand of Benin Formation consists of massive, highly porous sandstones with a few minor shale interbeds indicating an alluvial depositional

**Table 1.** The available well logs for the research and their principle uses.

| Well log                   | Log type           | Well 1 | Well 2 | Well 5 |
|----------------------------|--------------------|--------|--------|--------|
| Lithology/correlation logs | GR                 | **     | **     | **     |
|                            | SP                 | **     | **     | **     |
| Resistivity logs           | Laterolog          | --     | --     | --     |
|                            | Lateral            | --     | --     | --     |
|                            | Short normal       | --     | --     | --     |
|                            | Long normal        | **     | **     | **     |
|                            | Spherical focussed | --     | --     | --     |
|                            | Medium induction   | --     | --     | --     |
|                            | Deep induction     | --     | --     | --     |
| Porosity log               | Sonic              | **     | --     | --     |
|                            | Neutron            | **     | --     | **     |
|                            | Density            | --     | --     | **     |
| Caliper                    |                    | --     | --     | **     |

\*\* Available; --, not available.

environment. Though minor oil shows have been reported in Benin Formation, the formation is generally fresh water bearing and it is the main source of potable groundwater in the Niger Delta area.

The most striking structural styles of the Cenozoic Niger Delta complex are the syn-sedimentary structures which deform the delta beneath the Benin continental sand facie. The structures, regarded as the products of gravity sliding during the deltaic sedimentation, are polygenic in nature and their complexity increases generally in down delta direction (Merki, 1972). These syn-sedimentary structures are called growth faults which are predominantly trending NE to SW and NW to SE (Hosper, 1971). Rollover anticlines, shale ridges and diapers resulting from the upheaval ridges are the associated structures to the growth faults. The predominant structural trapping mechanisms for oil and gas within the study area are roll over anticlines and fault closures. The stratigraphic traps below unconformity surfaces include the paleo-channel fills, crestal accumulations, sand pinch-outs and erosional truncations, nonetheless above the unconformity surfaces are incised valley and lowstand fans (Orife and Avbovbo, 1981).

## METHODOLOGY

### Seismic and well logs data

The data used for this study are 3D seismic sections, composite geophysical well log suites and checkshot (for time-to-depth conversion). The 3D seismic reflection data comprise 637 inlines with interval of 25 m and 595 crosslines with interval of 25 m which covers an area of 102 km<sup>2</sup>. The number of samples per trace is 1251 with the sample interval of 4 mS. The reflection quality of the

seismic data was improved by applying structural smoothening volume attributes to suppress the noise so that faults and stratigraphic picks for the horizons are easily recognizable on the time section. The geophysical well logs (Table 1) for wells 1, 2 and 5 were available for this study (Figure 3); however, only wells 1 and 5 were used for the quantification of petrophysical attributes as porosity logs for well 2 were not available.

### Horizons and fault mapping

The gamma ray and resistivity logs were used for lithologic identification, well correlation, and reservoirs zonation. The 3D seismic reflection data was also utilized to study the hydrocarbon trapping styles within the entire field through identification and mapping of Faults and horizons at step intersection plane of 10 across both the inlines and crosslines of the seismic sections. Four (4) hydrocarbon bearing zones R1, R2, R3 and R4 were identified and correlated (Figure 4). The overlay of the four (4) horizons with the drilled wells is displays in Figure 5. The sand units in Niger Delta are regarded as the reservoir units because shale formations are not porous enough to retain and release fluid. Therefore in the reservoir sand units delineated, differentiation between reservoir fluids (hydrocarbon and water) was done using the resistivity log (Schlumberger, 1989). The tops of the identified reservoirs across the wells were tied to the seismic sections for identification and mapping of horizons using the checkshot data from the wells (Figure 5). The horizons were mapped/tracked on these seismic reflections, mapping both inline and crossline seismic sections across the entire field to produce the time structure (isochrones) maps. The derived velocity information from the checkshot data was used to generate the depth structure maps from the time structure maps.

### Petrophysical evaluation

Different mathematical models and relations were employed for quantitative interpretation of the well logs to estimate petrophysical parameters. Shale volume estimation ( $V_{sh}$ ) was calculated using

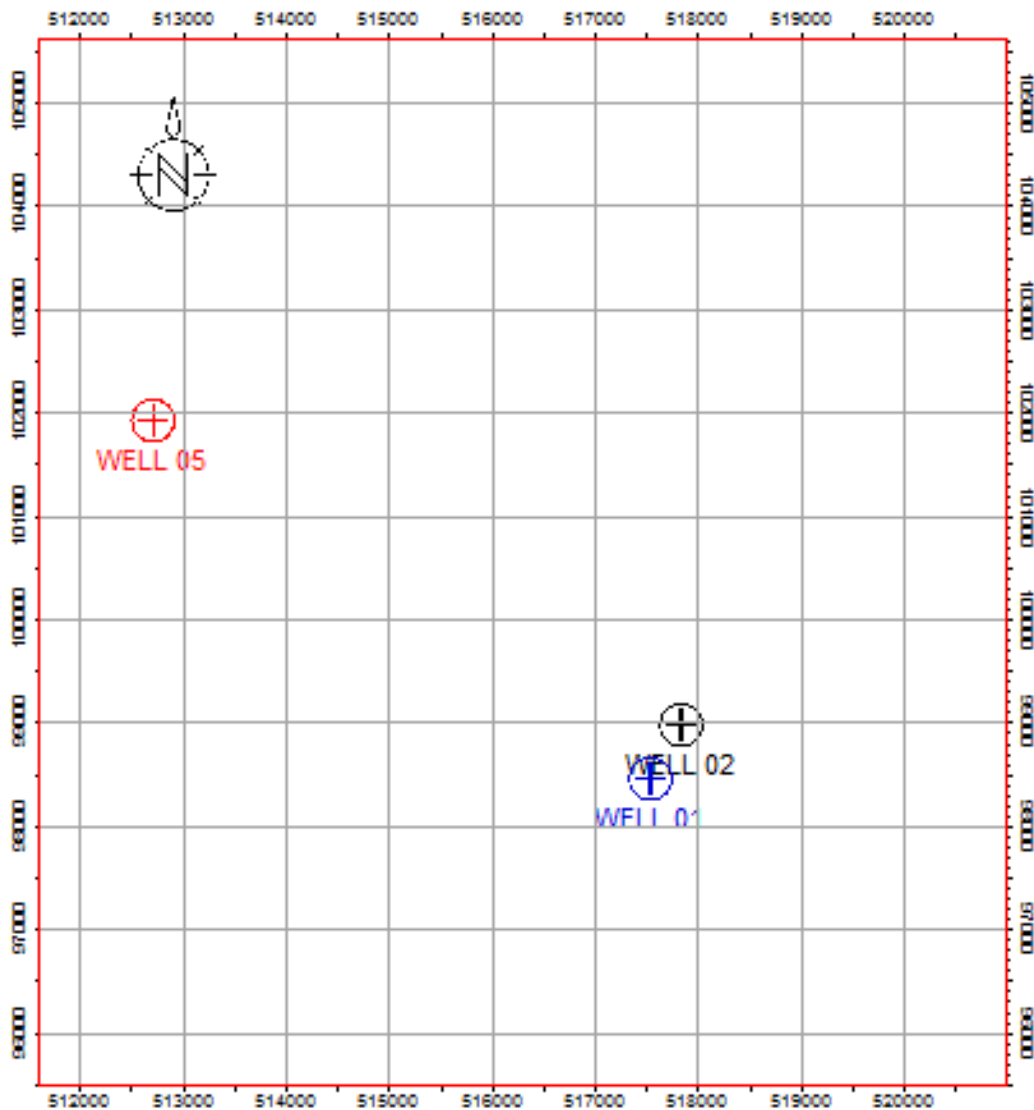


Figure 3. Basemap showing the locations of wells.

the Larionov's (1969) relation for tertiary rocks after gamma ray index  $I_{GR}$  (Schlumberger, 1974) was determined as follows:

$$V_{sh} = 0.083 [2^{(3.7 * I_{GR})} - 1.0] \tag{1}$$

Where:

$$I_{GR} = \frac{GR_{log} - GR_{min}}{GR_{max} - GR_{min}} \tag{2}$$

Porosity values for the hydrocarbon reservoirs were estimated. The amount of pore spaces or voids in the rock is a measure of the amount of fluid (notably, water, oil or gas) the rock will hold. The porosity log utilized was the bulk density log which records only the bulk density of the formation; therefore, density porosity was estimated using Asquith equation (Asquith, 2004) for the intervals of interest (hydrocarbon bearing intervals). The porosity from the sonic

log is given as:

$$\phi = \frac{\Delta t - \Delta t_{ma}}{\Delta t_f - \Delta t_{ma}} \tag{3}$$

where  $\phi$  is the porosity,  $\Delta t$  is the log reading in microseconds/foot ( $\mu s/ft$ ),  $\Delta t_f$  is the transit time for liquid filling the pore and  $\Delta t_{ma}$  is the transit time for the rock type matrix comprising the formation. The porosity derived from the density log is given as:

$$\phi_D = \frac{\rho_{ma} - \rho_b}{\rho_{ma} - \rho_f} \tag{4}$$

where  $\phi_D$  is the apparent density porosity,  $\rho_{ma}$  is the matrix density,  $\rho_b$  is the bulk density and  $\rho_f$  is the fluid density. The

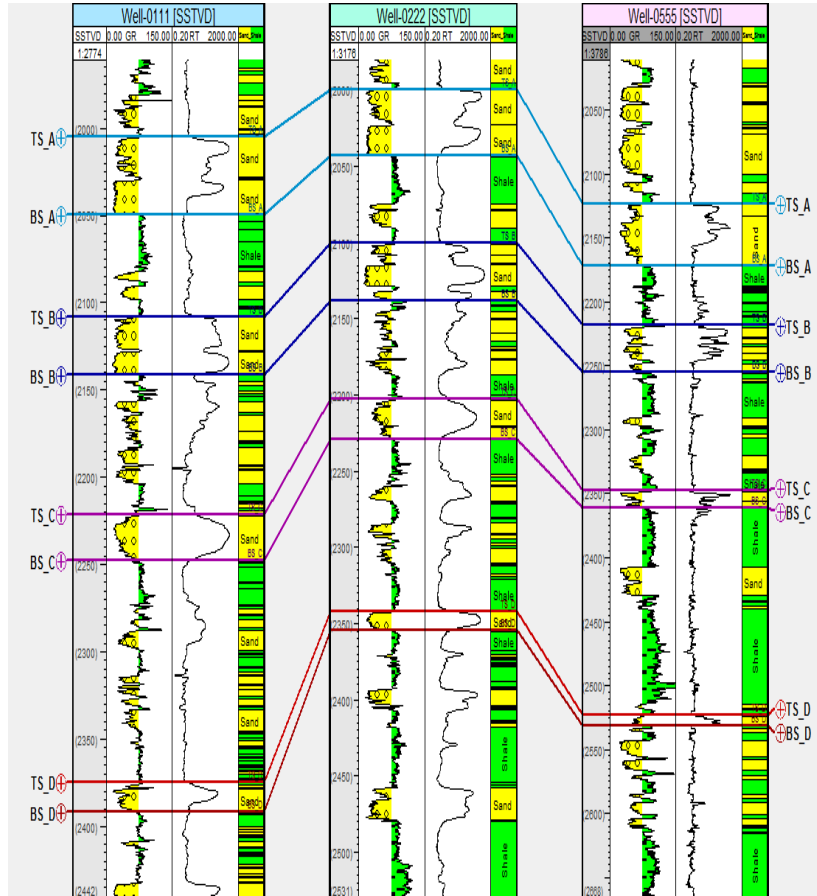


Figure 4. Well section window showing the reservoir zonation and correlation.

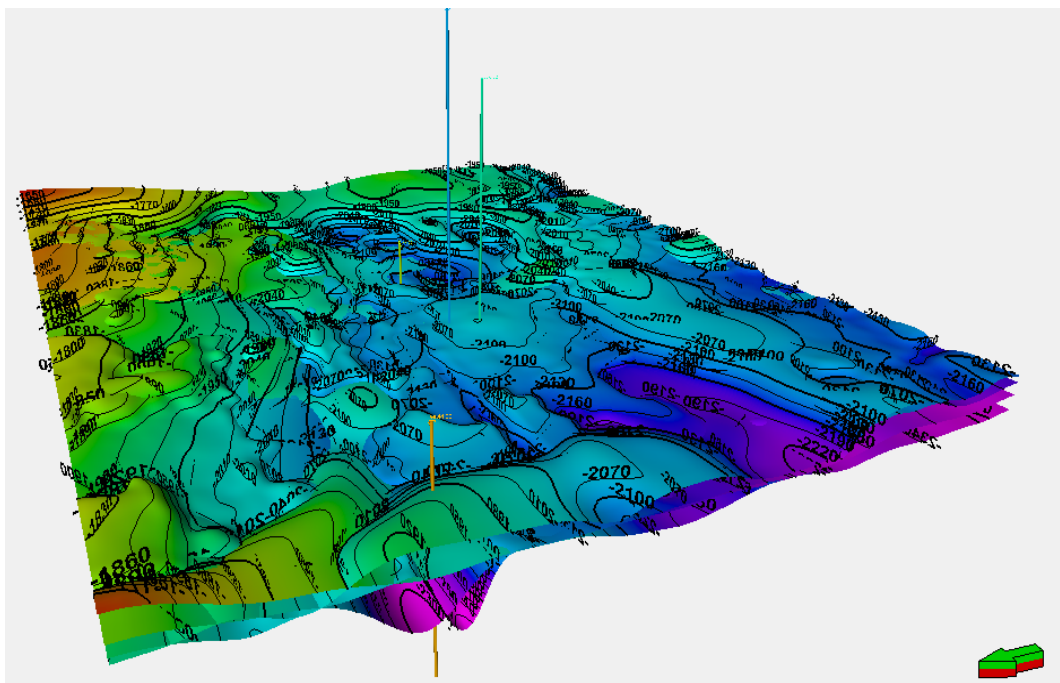


Figure 5. Overlay of the four (4) time structure maps and the wells.

effective porosity was estimated using the relation:

$$\phi_{eff} = (1 - V_{sh}) \times \phi \quad (5)$$

where  $V_{sh}$  is the volume of shale and  $\phi_{eff}$  is the effective porosity.

The formation factor is calculated as:

$$F = \frac{R_o}{R_w} \quad (6)$$

where  $F$  is the formation resistivity factor or formation factor,  $R_o$  is the resistivity of the rock when water saturation is 1 and  $R_w$  is the formation water resistivity. The formation factor can also be calculated as:

$$F = \frac{a}{\phi^m} \quad (7)$$

where  $F$  is the formation factor,  $a$  is the tortuosity factor,  $\phi$  is the porosity and  $m$  is the cementation exponent or factor. To calculate water saturation,  $S_w$  of uninvaded zone, the method used requires a water resistivity  $R_w$  value at formation temperature calculated from the porosity and resistivity logs within clean water zone using Equation (8). The water saturation was calculated using Equation (9) obtained from Archie's method:

$$R_w = \frac{\phi^m R_o}{a} \quad (8)$$

$$S_w = \sqrt{\frac{a \times R_w}{\phi^m \times R_t}} \quad (9)$$

where  $S_w$  is the water saturation and  $R_t$  is the true formation resistivity. Hydrocarbon Saturation  $S_h$  is the percentage of pore volume in a formation occupied by hydrocarbon. It can be determined by subtracting the value obtained for water saturation from 100% as:

$$S_h = (100 - S_w) \% \quad (10)$$

Bulk volume of water was evaluated using Equation (11). It shows whether a formation is at irreducible water saturation or not. For instance, if the estimated BVW values at several depths within a formation are coherent, then the zone is considered homogeneous and is at irreducible water saturation. Morris and Briggs (1967) opined that production from such zone should be water free.

$$BVW = S_w \times \phi \quad (11)$$

Permeability ( $K$ ), the property of a rock to transmit fluids was estimated for each reservoirs using Timur's model expressed as:

$$K = \frac{a \phi^b}{S_{wirr}^2} \quad (12)$$

Where  $\phi$  is the porosity,  $S_{wirr}$  is the irreducible water saturation,  $a$  is given as 0.136 and  $b$  is given as 4.4, if the values of the porosity and irreducible water saturation are in percentage.

## RESULTS AND DISCUSSION

### Structures and hydrocarbon prospects

The well-to-seismic match is shown in Figure 6. Figure 6 shows the four (4) hydrocarbon bearing reservoirs (R1, R2, R3, and R4) that were delineated and three (3) principal major faults ( $F_1$ ,  $F_2$  and  $F_4$ ) that were mapped along with other intermediate faults ( $F_3$  and  $F_6$ ) and minor faults ( $F_7$  and  $F_8$ ) using the variance edge structural seismic attributes (Figure 7). The structure maps and seismic sections revealed that the probable principal structure responsible for the hydrocarbon entrapment in the field is the anticlinal structure at the centre of the field which is tied to the crest of the rollover structure assisted by faults. The depth structure maps (Figures 13 to 16) were generated from the time structure maps (Figures 8 to 11) using the time-depth conversion curve (Figure 12) and revealed three (3) major Faults. The field is characteristically associated with large faults closures ("X" and "Y") against a series of down-to-south growth faults. The main body of the field is dissected by several intermediate faults which are majorly synthetic and antithetic faults.  $F_1$ ,  $F_2$  and  $F_4$  are thought to be the growth faults while  $F_7$  and  $F_8$  are both interpreted to be antithetic and synthetic faults respectively. Structural highs like diapiric structures (Figure 6) are observed in the field which perhaps constitute the structural traps for hydrocarbon.

### Petrophysical analysis

The wireline logs expedite the evaluation of the field's petrophysical attributes. The lithologic identification along with well logs correlation was achieved using gamma ray (GR) log (Figure 4) and the major lithologies encountered in the study area were basically shale and sand, some of which occur as interbeds. It was noted that the shale units serves as seal to the reservoir sand units. Table 2 shows details of the four (4) stratigraphic zones correlated across Wells 01, 02 and 05. Lithological characterization for each identified reservoir comprising their gross thickness, net-gross ratio and shale streak across Wells 01 and 02 are presented in Tables 3 and 4. The reservoir sand units were evaluated quantitatively for petrophysical properties such as porosity, water saturation, shale volume, hydrocarbon saturation and permeability. The summary of these estimated attributes towards formation evaluation analysis are presented in Tables 5 and 6. Porosity values for the entire mapped surface are very good according to Levorsen (1967) with

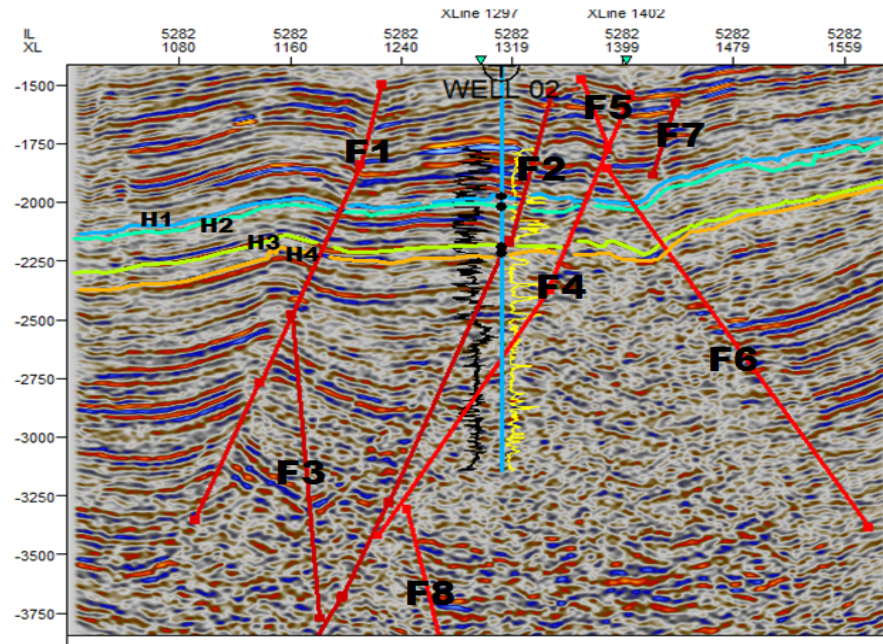


**Figure 6.** Well - to - seismic tie showing mapped faults and horizons.

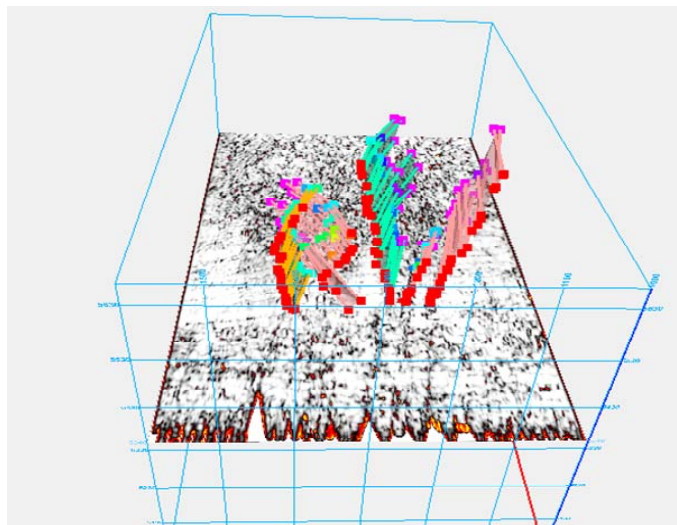
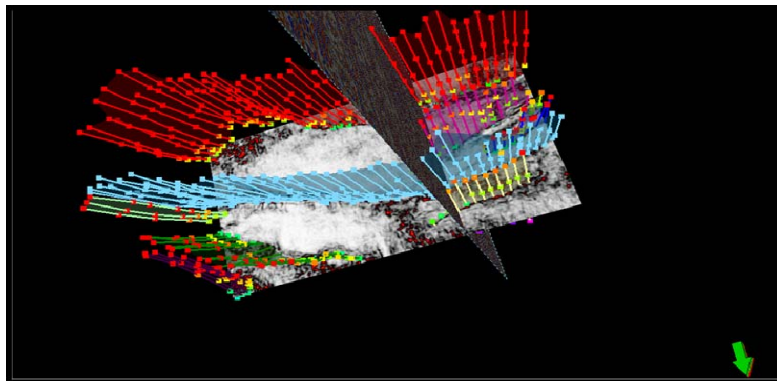


**Figure 7.** Variance edge attributes displaying mapped faults.

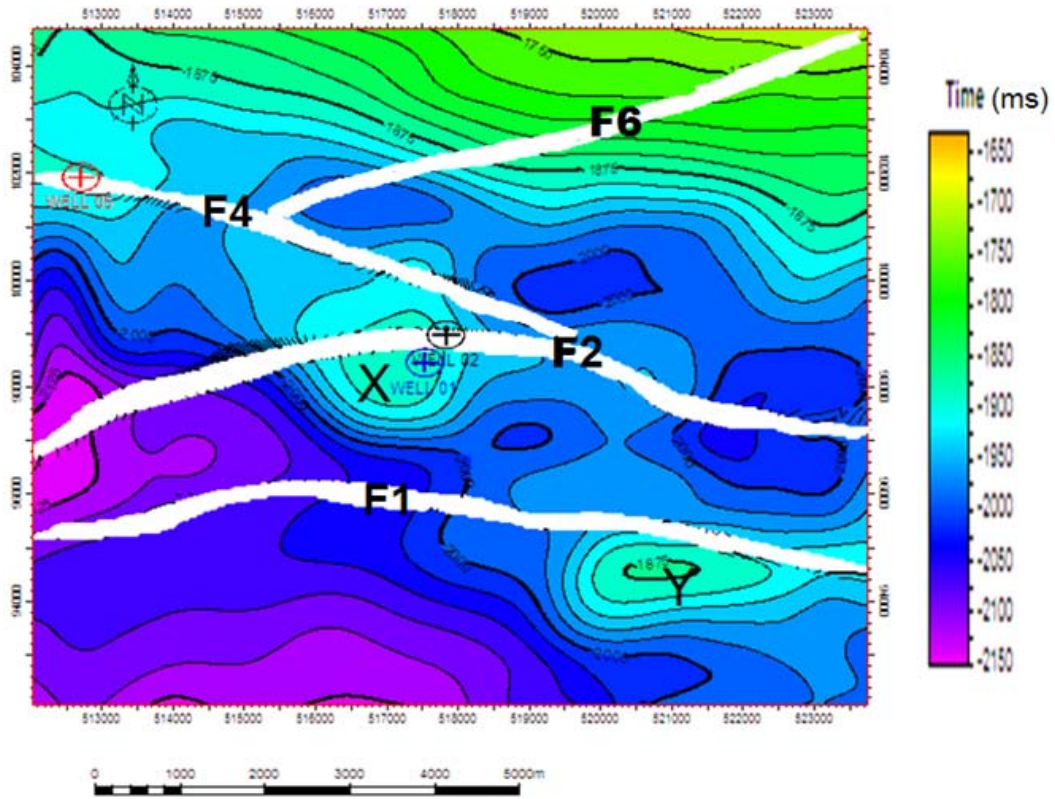


Figure 8. Time structure map of horizon R1.

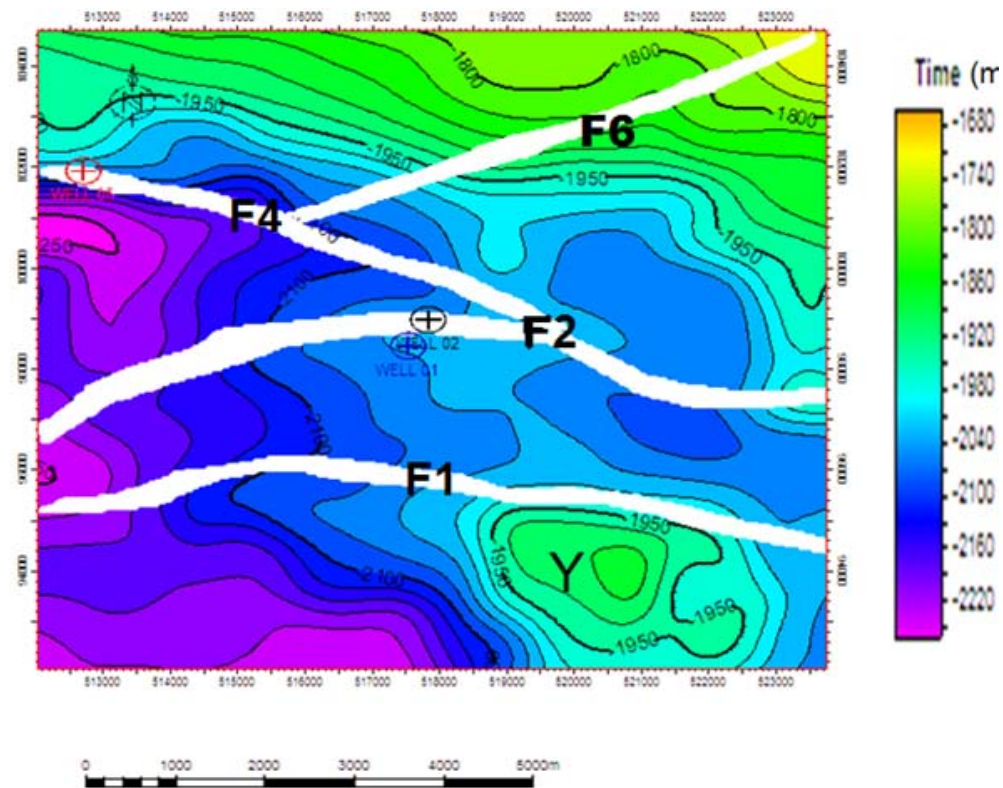


Figure 9. Time structure map of horizon R2.

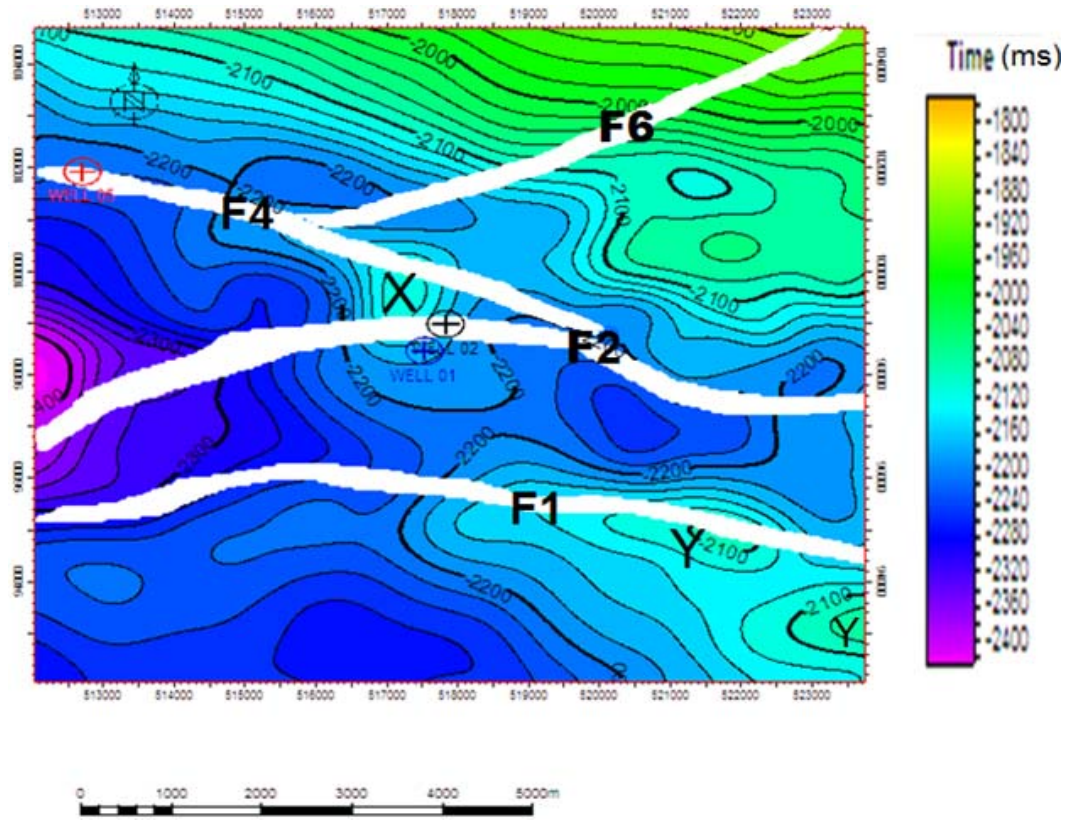


Figure 10. Time structure map of horizon R3.

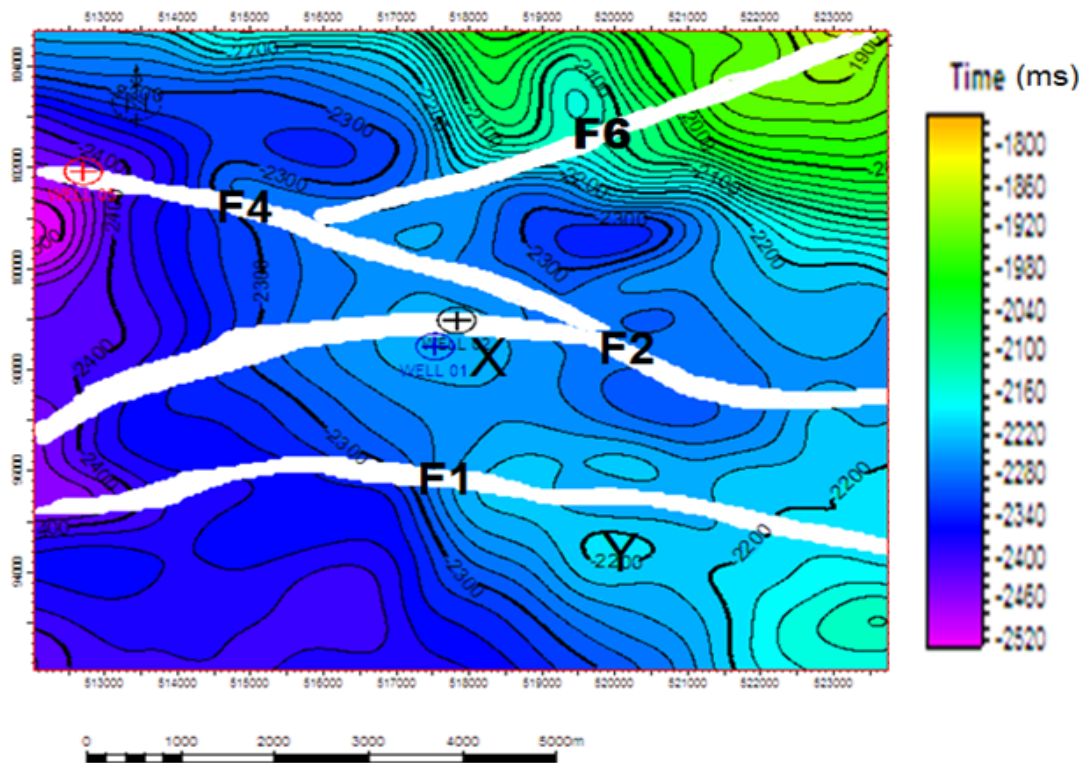


Figure 11. Time structure map of horizon R4.

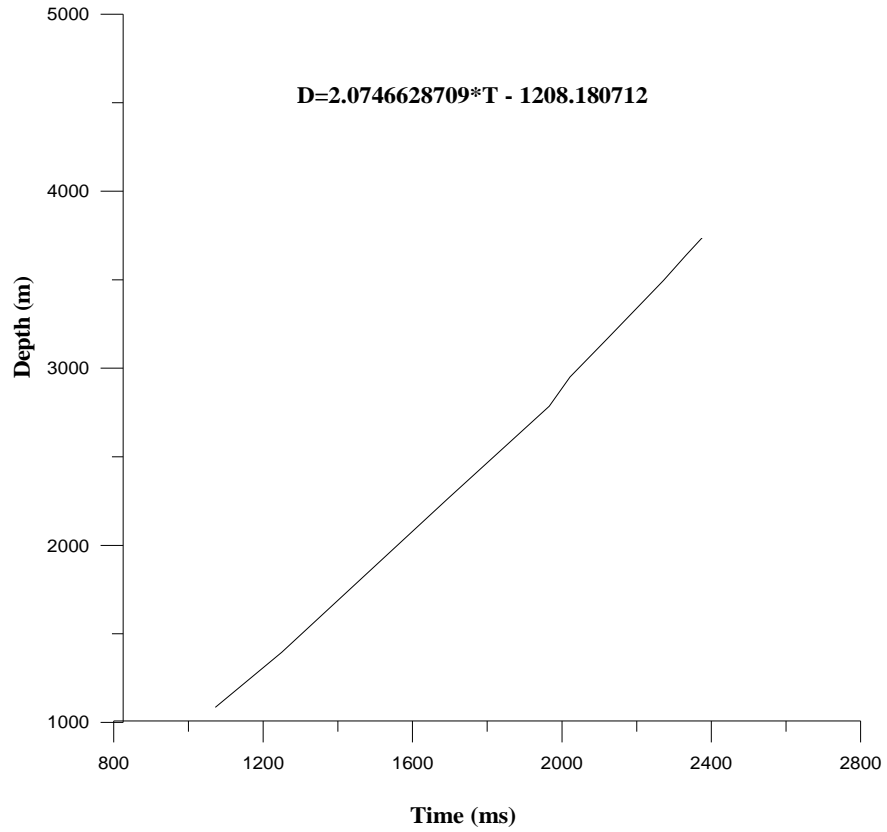


Figure 12. Time to depth conversion curve for Well 1.

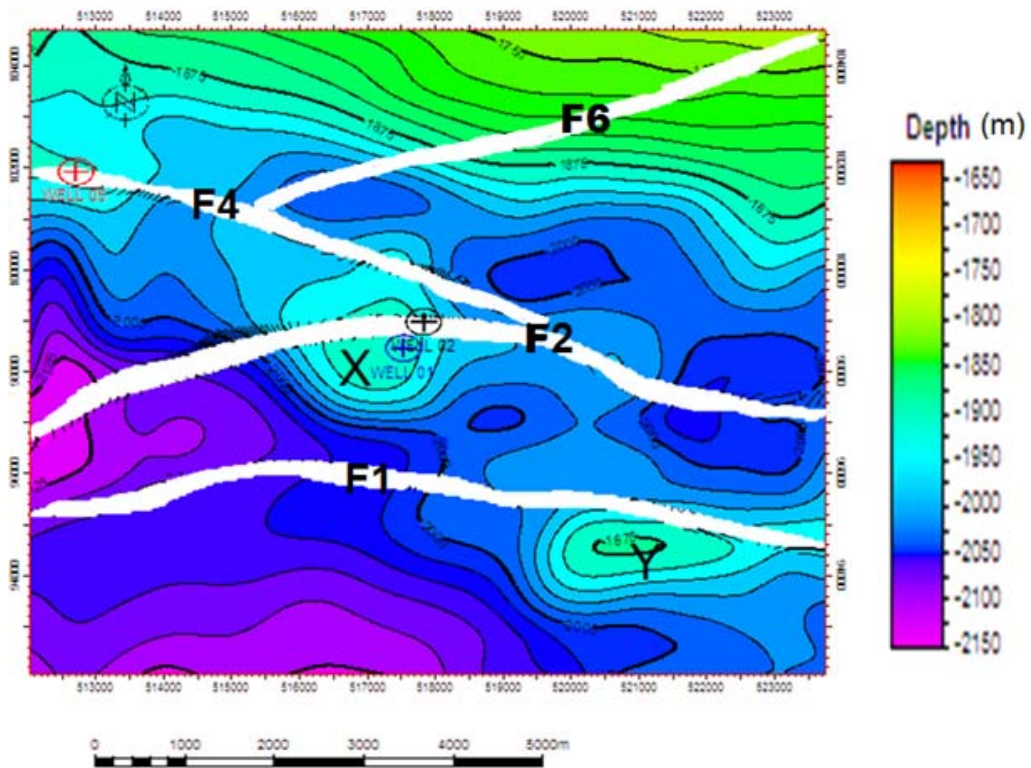


Figure 13. Depth structure map of horizon R1.

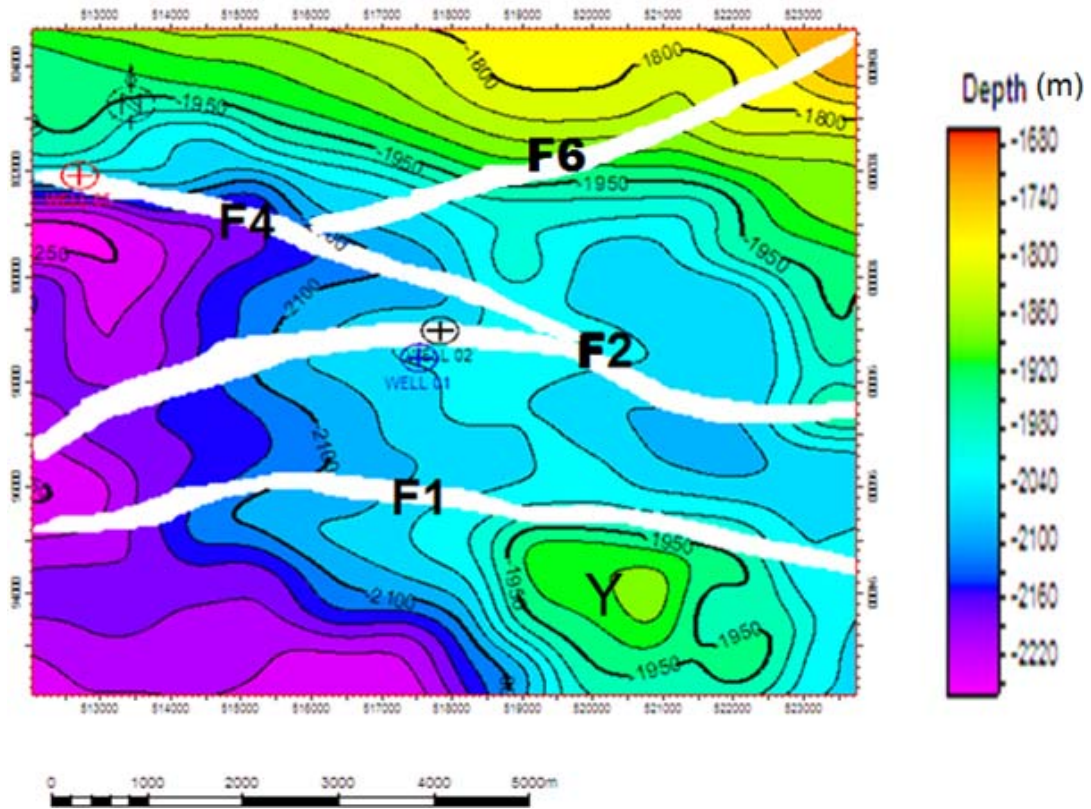


Figure 14. Depth structure map of horizon R2.

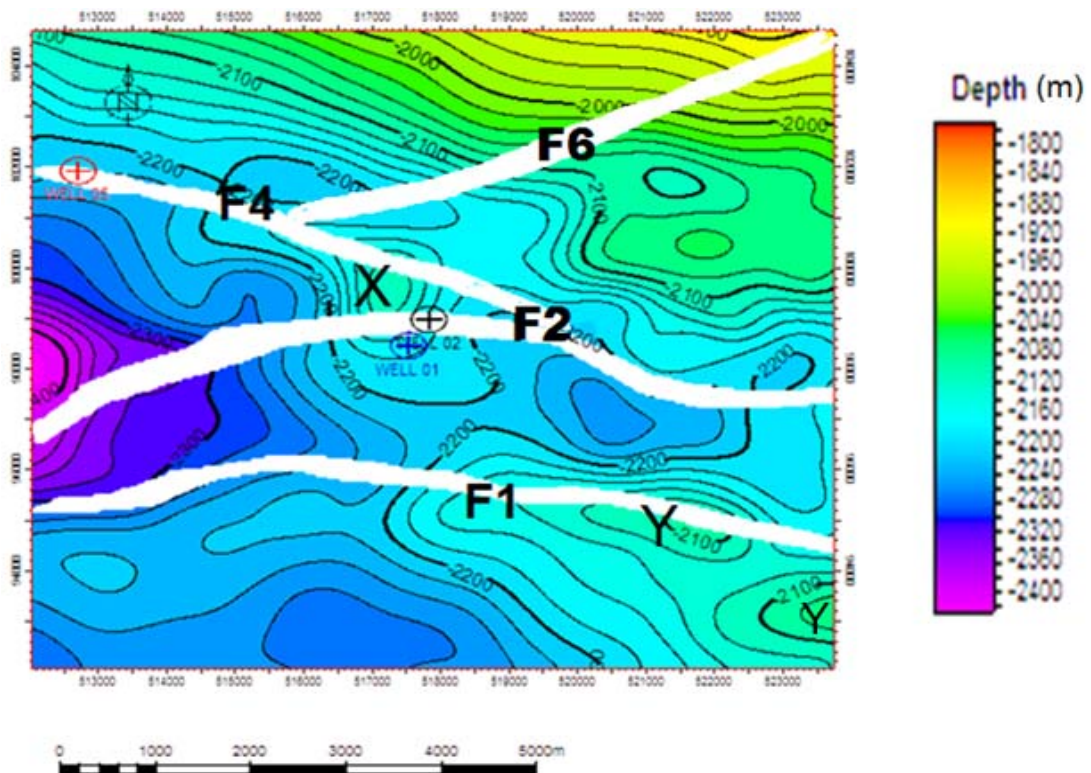


Figure 15. Depth structure map of horizon R3.

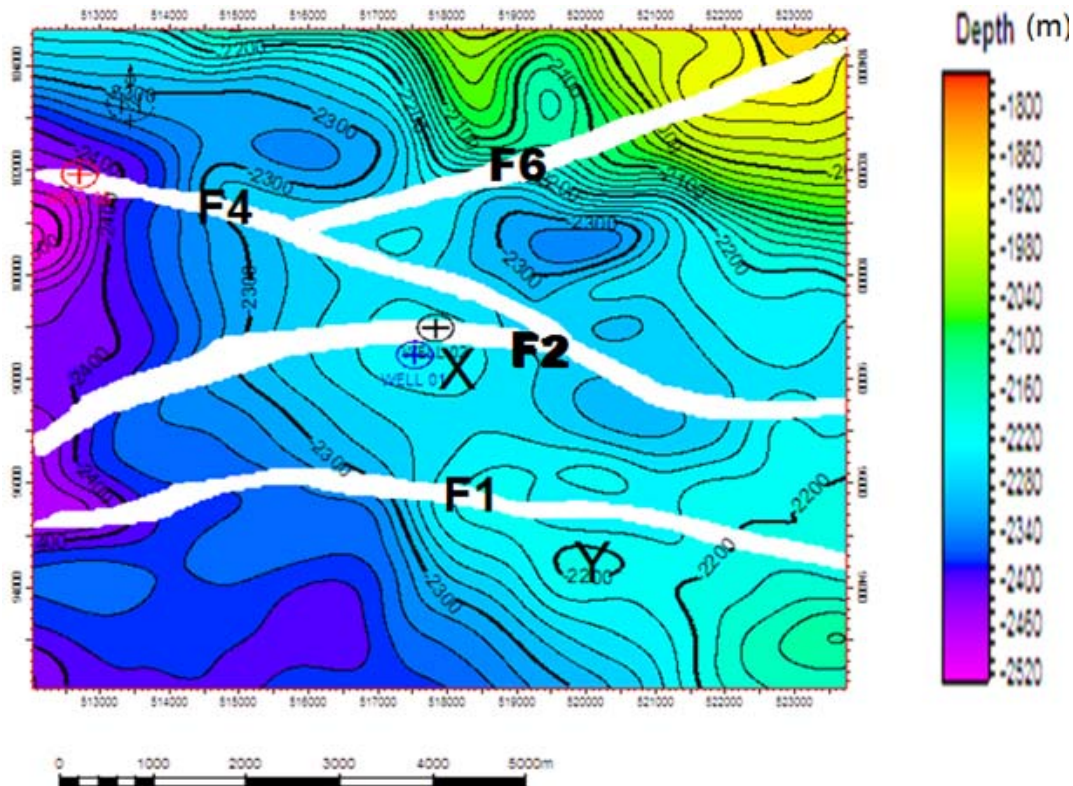


Figure 16. Depth structure map of horizon R4.

Table 2. The stratigraphic reservoir zones from well correlation.

| Reservoirs | Well 1 top-base (ft) | Well 2 top-base (ft) | Well 5 top - base (ft) |
|------------|----------------------|----------------------|------------------------|
| R1         | 2004.90 - 2049.62    | 2000.02 - 2043.27    | 2123.14 - 2171.74      |
| R2         | 2108.13 - 2141.31    | 2100.28 - 2138.20    | 2218.28 - 2254.73      |
| R3         | 2222.18 - 2247.62    | 2208.53 - 2229.13    | 2347.88 - 2361.06      |
| R4         | 2374.73 - 2391.71    | 2342.02 - 2354.40    | 2523.00 - 2531.10      |

Table 3. Lithological identification of Well 1.

| Reservoir name | Top     | Base    | Thickness (gross) | Shale streak | Thickness (net) | Net/gross | Net/gross (%) |
|----------------|---------|---------|-------------------|--------------|-----------------|-----------|---------------|
| R1             | 2000.4  | 2049.62 | 49.22             | 4.11         | 45.11           | 0.9165    | 91.65         |
| R2             | 2108.4  | 2141.31 | 33.18             | 2.77         | 30.41           | 0.9165    | 91.65         |
| R3             | 2222.18 | 2247.62 | 25.44             | 5.91         | 19.53           | 0.7677    | 76.77         |
| R4             | 2374.73 | 2391.71 | 16.98             | 3.08         | 13.9            | 0.8186    | 81.86         |

Table 4. Lithological identification of Well 5.

| Reservoir name | Top     | Base    | Thickness (gross) | Shale streak | Thickness (net) | Net/gross | Net/gross (%) |
|----------------|---------|---------|-------------------|--------------|-----------------|-----------|---------------|
| R1             | 2123.14 | 2171.74 | 48.6              | 3.82         | 44.78           | 0.9214    | 92.14         |
| R2             | 2218.28 | 2254.73 | 36.45             | 3.65         | 32.80           | 0.8999    | 89.99         |
| R3             | 2347.88 | 2361.06 | 13.18             | 2.05         | 11.13           | 0.8445    | 84.45         |
| R4             | 2523.00 | 2531.10 | 8.10              | 2.54         | 5.56            | 0.6864    | 68.64         |

**Table 5.** Summary of Petrophysical attributes at Well 1.

| Reservoir name | Depth interval  | Reservoir thickness | $V_{Sh}$ (%) | $R_t$   | $R_w$  | $\phi$ (%) | F     | $S_{gr}$ (%) | BVW (%) | $S_{wirr}$ (%) | K (mD)   | $S_h$ (%) |
|----------------|-----------------|---------------------|--------------|---------|--------|------------|-------|--------------|---------|----------------|----------|-----------|
| R1             | 2004.90-2049.62 | 49.22               | 8.59         | 333.000 | 0.0189 | 24.5       | 13.5  | 3.07         | 0.75    | 8.22           | 2606.91  | 96.93     |
| R2             | 2108.13-2141.31 | 33.18               | 7.03         | 242.362 | 0.1337 | 24.5       | 13.5  | 9.59         | 2.35    | 8.22           | 2606.91  | 90.41     |
| R3             | 2222.18-2247.62 | 25.44               | 10.20        | 482.148 | 0.2091 | 31.0       | 8.43  | 6.72         | 2.08    | 6.49           | 11777.71 | 93.28     |
| R4             | 2374.73-2391.71 | 16.98               | 26.56        | 93.460  | 0.0949 | 26.5       | 11.54 | 12.02        | 3.19    | 7.60           | 4307.19  | 87.98     |

**Table 6.** Summary of Petrophysical attributes at Well 5.

| Reservoir name | Depth interval  | Reservoir thickness | $V_{Sh}$ (%) | $R_t$ ( $\Omega m$ ) | $R_w$ ( $\Omega m$ ) | $\phi$ (%) | F     | $S_{gr}$ (%) | BVW (%) | $S_{wirr}$ (%) | K (mD)  | $S_h$ (%) |
|----------------|-----------------|---------------------|--------------|----------------------|----------------------|------------|-------|--------------|---------|----------------|---------|-----------|
| R1             | 2123.14-2171.74 | 48.6                | 12.83        | 177.737              | 0.1468               | 27.75      | 10.52 | 10.36        | 2.87    | 7.25           | 5797.22 | 89.64     |
| R2             | 2218.28-2254.73 | 36.45               | 8.17         | 181.480              | 0.1344               | 28.25      | 10.15 | 9.63         | 2.72    | 7.12           | 6502.20 | 90.37     |
| R3             | 2347.88-2361.06 | 13.18               | 16.47        | 316.325              | 0.0919               | 23.50      | 14.67 | 7.25         | 1.70    | 8.56           | 2001.40 | 92.75     |
| R4             | 2523.00-2531.10 | 8.10                | 11.01        | 54.970               | 0.0927               | 21.25      | 17.92 | 19.32        | 4.11    | 9.47           | 1050.07 | 80.68     |

a range of 24.5 to 31% in Well 1 and 21.25 to 28.25% in Well 5, water saturation is 3.07 to 12.02% in Well 1 and 7.25 to 19.32% in Well 5, hydrocarbon saturation 87.98 to 96.93% in Well 1 and 80.68 to 92.75% in Well 5. The permeability which is the ability of the reservoir formations to transmit fluid ranged between 2606.91 to 11,777.71 mD in Well 1, 1050 to 6502.20 mD in Well 5 making the reservoir sand highly productive. Figures 18 to 21 compare the petrophysical parameters for each mapped reservoir between Wells 01 and 05. Neutron density logs were used to define hydrocarbon type present in Afam Field. The combination of neutron and density logs was used for reservoir in both wells to detect gas zone (Figure 17). At these intervals, density porosity was observed to be greater than neutron porosity and the curves crossover each other, therefore were identified as gas bearing zones.

The results of these petrophysical attributes analysis revealed the presence of hydrocarbon in

the four correlated reservoir sand units at quantities favourable for commercial exploitation with R4 having the highest average hydrocarbon saturation. The high values of the estimated porosity and permeability denote that the reservoir sand units are well sorted. The evaluated petrophysical parameters are in line with that of other researchers (Edwards and Santagrossi, 1990; Anyiam et al., 2010; Olowokere and Ojo, 2011; Aigbedion and Aigbedion, 2011). The variations in the porosity of the reservoir units across the Niger Delta basin could be ascribed to the differential volume of shale in the reservoirs. These petrophysical properties obtained are the parameters required for estimating the hydrocarbon in place.

### Conclusion

The subsurface geology, hydrocarbon structural trapping mechanism and petrophysical attributes

evaluation of Afam field, offshore Niger Delta have been studied using 3D seismic and composite well logs. The major and minor faults were delineated and mapped confirming the area to be highly faulted, typical of the tectonic setting of Niger Delta. Reservoir sand units marked R1, R2, R3 and R4 were mapped out based on log curve signatures of the gamma ray log, neutron log, formation density log, and resistivity logs. They were correlated across the wells and hydrocarbon intervals in Afam field were mapped on to the seismic section for well-to-seismic tie using time-depth data. The mapped horizons on the well logs suite were picked across the inlines and the crosslines, within the time window of 2126 and 2326 mS of the seismic section. Time and depth structural maps of these surfaces were also generated to study the geometry of the structure trapping oil and gas in the field. Depth maps by average velocity gave the various depth to the surface mapped. Trapping mechanism in Afam field were also revealed to be the anticlinal

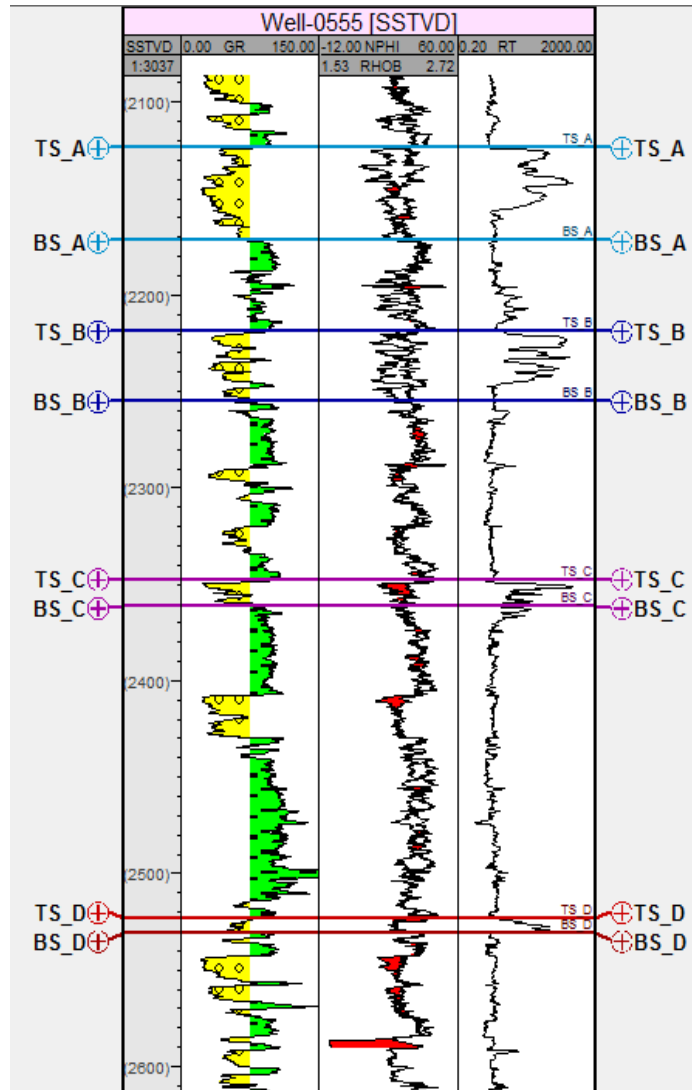


Figure 17. Hydrocarbon type identifications using neutron and density logs.

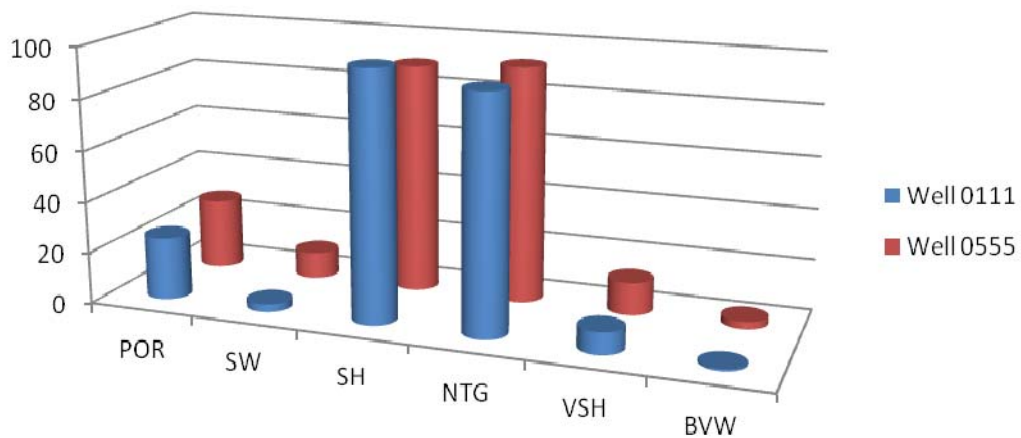
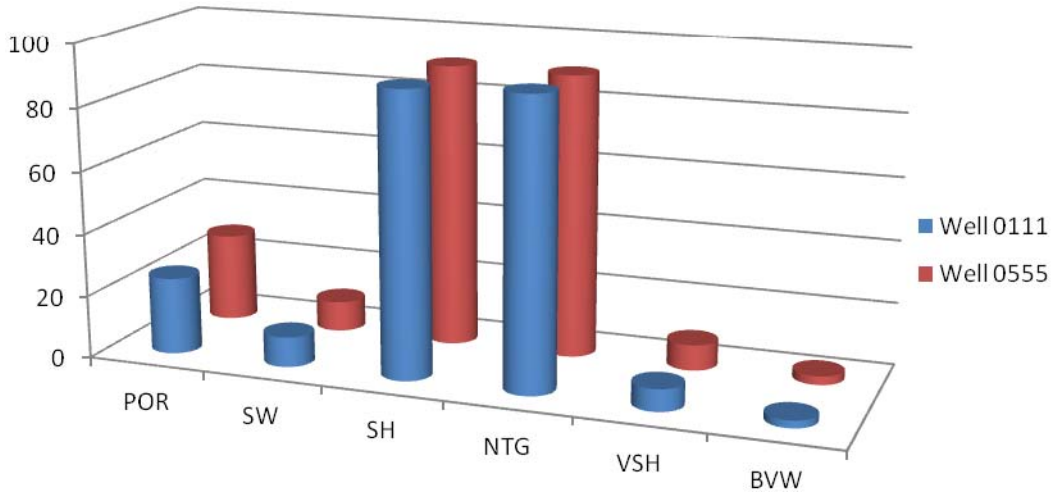
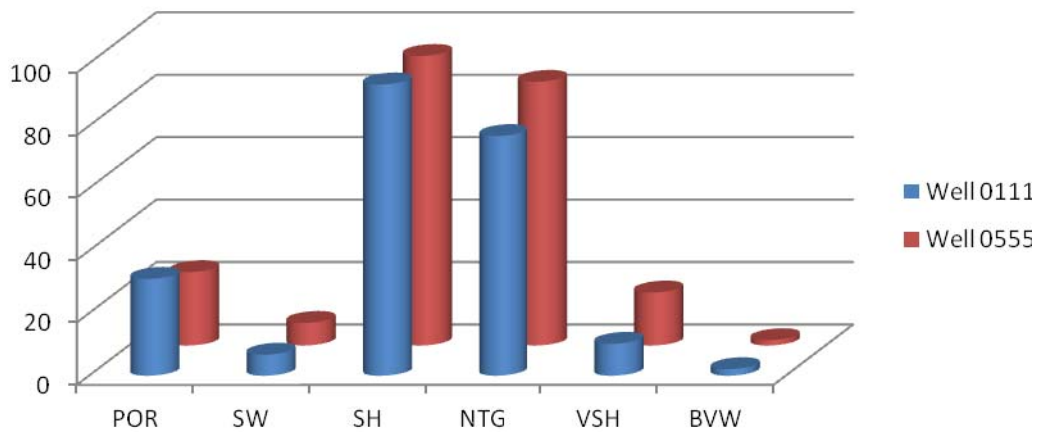


Figure 18. Chart showing relationship between percentage porosity, water saturation, hydrocarbon saturation and net/gross, volume of shale and bulk volume of water for R1.



**Figure 19.** Chart showing relationship between percentage porosity, water saturation, hydrocarbon saturation and net/gross, volume of shale and bulk volume of water of R2.



**Figure 20.** Chart showing relationship between percentage porosity, water saturation, hydrocarbon saturation and net/gross, volume of shale and bulk volume of water for R3.

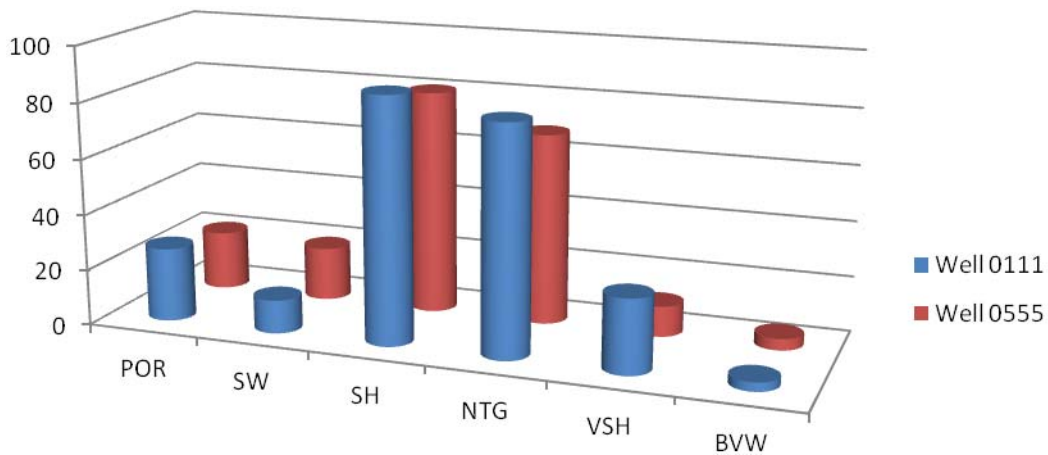


**Figure 21.** Chart showing relationship between percentage porosity, water saturation, hydrocarbon saturation and net/gross, volume of shale and bulk volume of water for R4.

structure at the centre of the field which is tied to the crest of the rollover structure assisted by faults and also largely by means of fault assisted closures (X and Y). The two way closure "Y" about SE section of the depth structure map is localized close to a fault and can consequently acts as a seal to further improve the integrity of the fault. The reservoir sand units were evaluated quantitatively for petrophysical attributes e.g. porosity, water saturation net pay, volume of shale, formation factor, irreducible water saturation, bulk water volume, permeability fluid content determinations and fluid contact. Neutron density logs were used to define hydrocarbon type present in Afam Field. Porosity values are between 21.25 and 31% for the mapped hydrocarbon bearing sand units which are productive reservoirs units. The hydrocarbon saturation of all the reservoir zones ranges from 80.68 to 96.93%. High resistivity  $R_t$ , porosity and permeability values in the entire hydrocarbon bearing reservoir zones were observed from the petrophysical data.

### Conflict of Interest

The authors have not declared any conflict of interest.

### REFERENCES

- Aigbedion I, Aigbedion HO (2011). Hydrocarbon volumetric analysis using seismic and Borehole data over Umoru Field, Niger Delta-Nigeria. *Int. J. Geosci.* 2:179-183.
- Anyiam U, Nduka V, Opara AI (2010). 3-D Seismic interpretation and reserve estimation of Ossu Field in OML 124, Onshore Niger Delta Basin, Nigeria. *SEG Denver Annual Meeting* pp.1327-1330.
- Asquith G (2004). *Basic Well Log Analysis*. AAPG, Methods in exploration series. 16:12-135.
- Biddle KT, Wielchowsky CC (1994). Hydrocarbon traps, in, Magoon LB, Dow WG, eds., *The Petroleum System- From Source to Traps*. AAPG Memoir. 60:219-235.
- Clapp FG (1929). Role of geologic structure in accumulations of petroleum, structure of typical American oil fields. *AAPG Bulletin.* 2:667-716.
- Doust H, Omatsola EM (1990). Niger Delta, in, Edwards and Santogrossi Eds., *Divergent/Passive Margin Basins*. AAPG Memoir 48:201-238.
- Edwards JD, Santagrossi PA (1990). Summary and Conclusions, in, Edwards and Santogrossi Eds., *Divergent/Passive Margin Basins*. AAPG Memoir. 48:239-248.
- Harding TP, Lowell JD (1979). Structural styles, their plate tectonics habitats, and hydrocarbon traps in petroleum province. *AAPG Bulletin.* 63:1016-1058.
- Hosper J (1971). The geology of the Niger Delta area, in, *The Geology of the East Atlantic Continental margin, Great Britain*. Inst. Geological Sci. Report 70(16):121-147.
- Larionov VV (1969). *Borehole Radiometry: Moscow, U.S.S.R. Nedra*.
- Levorsen AI (1967). *Geology of petroleum*. W.H. Freeman and Co., San Francisco, 2nd edition.
- Merki PJ (1972). Structural geology of the Cenozoic Niger Delta. 1st Conference on African Geology Proceedings, Ibadan University Press pp. 635-646.
- Morris RL, Briggs WP (1967). Using log-derived values of water saturation and porosity". *Trans. SPWLA Ann. Logging Symp.* Paper 10-26.
- North FK (1985). *Petroleum geology*. Allen and Unwin, Boston. <http://trove.nla.gov.au/work/18736333?q&versionId=45649908>
- Ojo AO (1996). Pre-drill prospect evaluation in deep water Nigeria. *Nig. Assoc. Petrol. Explo. Bull.* 11:11-22.
- Olowokere MT, Ojo JS (2011). Porosity and lithology prediction in Eve Field, Niger Delta using compaction curves and rock physics models. *Int. J. Geosci.* 2:366-372.
- Opara AI, Onuoha KM (2009). Pre-drill pore pressure prediction from 3-D seismic data in parts of the Onshore Niger Delta Basin. 33rd Annual SPE International Technical Conference and Exhibition in Abuja, Nigeria. SPE 128354.
- Orife JM, Avbovbo AA (1981). Stratigraphic and unconformity traps in the Niger Delta. *AAPG Bulletin.* 57:251-262.
- Perrodon A (1983). Dynamics of oil and gas accumulations. *Bulletin des Centres de Recherches Exploration-Production Elf-Aquitaine, Memoir.* P. 5.
- Reijers TJA (2011). Stratigraphy and sedimentology of the Niger Delta. *Geologos* 17(3):133-162.
- Schlumberger (1974). *Log Interpretation Charts*. Schlumberger Educational Services. New York. P. 83.
- Schlumberger (1989). *Log Interpretation, Principles and Application, Schlumberger Wireline and Testing*, Houston. Texas. pp. 21-89.
- Weber KJ, Daukoru EM (1975). *Petroleum geology of the Niger Delta*. Proc. of 9th world petroleum congress. Tokyo 2:209-221.